

## Bright source of cold ions for surface-electrode traps

Marko Cetina, Andrew Grier, Jonathan Campbell, Isaac Chuang, and Vladan Vuletić

*Department of Physics, MIT-Harvard Center for Ultracold Atoms, and Research Laboratory of Electronics,  
Massachusetts Institute of Technology, Cambridge, Massachusetts 02139, USA*

(Received 1 February 2007; published 24 October 2007)

We produce large numbers of low-energy ions by photoionization of laser-cooled atoms inside a surface-electrode-based Paul trap. The isotope-selective trap's loading rate of  $4 \times 10^5$  Yb<sup>+</sup> ions/s exceeds that attained by photoionization (electron-impact ionization) of an atomic beam by three (six) orders of magnitude. Traps as shallow as 0.13 eV are easily loaded with this technique. The ions are confined in the same spatial region as the laser-cooled atoms, which will allow the experimental investigation of interactions between cold ions and cold atoms or Bose-Einstein condensates.

DOI: [10.1103/PhysRevA.76.041401](https://doi.org/10.1103/PhysRevA.76.041401)

PACS number(s): 32.80.Pj, 03.67.Lx, 32.80.Fb, 34.70.+e

Among the many candidate systems for large-scale quantum-information processing, trapped ions currently offer unmatched coherence and control properties [1]. The basic building blocks of a processor, such as quantum gates [2], subspaces with reduced decoherence [3], quantum teleportation [4,5], and entanglement of up to eight ions [6,7] have already been demonstrated. Nevertheless, since a logical qubit will likely have to be encoded simultaneously in several ions for error correction [8,9], even a few-qubit system will require substantially more complex trap structures than currently in use. Versatile trapping geometries can be realized with surface-electrode Paul traps, where electrodes residing on a surface create three-dimensional confining potentials above it [10]. Such surface traps allow good optical access to the ions and can be fabricated using simpler lithographic techniques than three-dimensional traps [11–13].

While the prospect of scalable quantum computing has been the main motivation for developing surface-electrode traps, it is likely that this emerging technology will have a number of other important, and perhaps more immediate, applications. Porras and Cirac have proposed using dense lattices of ion traps, where neighboring ions interact via the Coulomb force, for quantum simulation [14]. A lattice with a larger period, to avoid ion-ion interactions altogether, could allow the parallel operation of many single-ion optical clocks [15], thereby significantly boosting the signal-to-noise ratio. The increased optical access provided by planar traps could be used to couple an array of ion traps to an optical resonator and efficiently map the stored quantum information onto photons [16]. Since the surface-electrode arrangement allows one to displace the trap minimum freely in all directions, ions can be easily moved through an ensemble of cold neutral atoms for investigations of cold-ion-atom-collisions [17–19], as proposed by Smith *et al.* [20]. One could even implant a single ion inside a Bose-Einstein condensate [21].

Compared to standard Paul traps [11–13], the open geometry of surface-electrode traps restricts the trap depth and increases the susceptibility to stray electric fields, making trap loading and compensation more difficult. Nevertheless, successful loading from a thermal atomic beam has recently been demonstrated using both photoionization [22] and electron-impact ionization aided by buffer gas cooling [23]. Photoionization, first demonstrated in Ref. [24], is superior in that it provides faster, isotope-selective loading

[22,25–27]. However, the loading rate  $R$  for microfabricated traps remains relatively low ( $R < 1$  s<sup>-1</sup> [11]), while charge-exchange collisions make it difficult to prepare large, isotopically pure samples even in macroscopic traps with  $R \sim 100$  s<sup>-1</sup> [26].

In this Rapid Communication, we demonstrate that large numbers of low-energy ions can be produced by photoionization of a laser-cooled, isotopically pure atomic sample, providing a robust and virtually fail-safe technique to load shallow or initially poorly compensated surface ion traps. We achieve a loading rate of  $4 \times 10^5$  Yb ions per second into a  $U_0 = 0.4$  eV deep printed-circuit ion trap, several orders of magnitude larger than with any other method demonstrated so far, and have directly loaded traps as shallow as  $U_0 = 0.13$  eV. The trapping efficiency for the generated low-energy ions is of order unity. We also realize a system where ions are confined in the same spatial region as laser-cooled atoms [20], allowing for future experimental studies of cold ion-atom collisions [17–19].

Efficient photoionization of Yb atoms is accomplished with a single photon from the excited  $^1P_1$  state that is populated during laser cooling, which lies 3.11 eV (corresponding to a 394 nm photon) below the ionization continuum. Due to momentum and energy conservation, most of the ionization photon's excess energy is transferred to the electron. Therefore, when we ionize atoms at rest even with 3.36 eV (369 nm) photons (the ion cooling light), the calculated kinetic energy of the ions amounts to only 8 mK (0.7  $\mu$ eV). Previously, excitation of cold atoms to high-lying Rydberg states has been used to generate and study cold but untrapped plasmas in the 1 K temperature range [32].

The ion trap is a commercial printed circuit on a vacuum-compatible substrate (Rogers 4350) with low radiofrequency (rf) loss. The three 1-mm-wide, 17.5- $\mu$ m-thick copper rf electrodes are spaced by 1-mm-wide slits (Fig. 1), whose inner surfaces are metallized to avoid charge buildup. Twelve dc electrodes placed outside the rf electrodes provide trapping in the axial direction and permit cancellation of stray electric fields. In addition, the rf electrodes can be dc biased to apply a vertical electric field. All dielectric surfaces outside the dc electrodes have been removed with the exception of a 500- $\mu$ m-wide strip supporting the dc electrodes.

The ratio between the rf voltages  $V_c$  and  $V_o$  applied to the

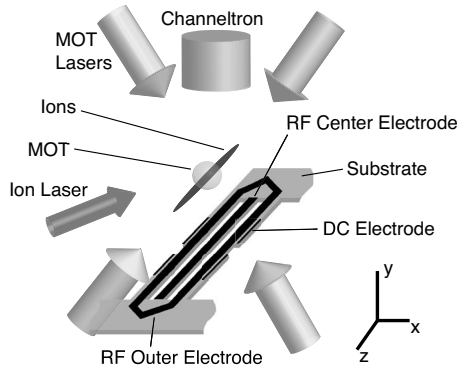


FIG. 1. Setup for loading a surface-electrode ion trap by in-trap photoionization of laser-cooled atoms. A  $^{172}\text{Yb}$  or  $^{174}\text{Yb}$  magneto-optical trap (MOT) is formed 4 mm above the trap surface. Cold  $\text{Yb}^+$  ions are produced inside the Paul trap by single-photon excitation from the excited  $^1P_1$  atomic state.

center and outer electrodes, respectively, determines the trap height above the surface. For  $V_c/V_o = -0.63$ , the rf node is located 3.6(1) mm above the surface. At a rf frequency of 850 kHz  $V_o = 540$  V yields a secular trap potential with a predicted depth of  $U_0 = 0.16$  eV (Fig. 2) and a calculated (measured) secular frequency of 100 kHz (90 kHz). The trap can be deepened by applying a static bias voltage  $V_{dc} < 0$  to all rf electrodes [23] and unbiased after loading (Fig. 2). This enables us to load traps with depths as small as  $U_0 = 0.13$  eV.

All Yb and  $\text{Yb}^+$  cooling, detection, and photoionization light is derived from near-uv external-cavity diode lasers. A master-slave laser system consisting of an external-cavity grating laser and an injected slave laser using violet laser diodes (Nichia) delivers 10 mW in three pairs of 3.4-mm-diameter beams for a magneto-optical trap (MOT) operating on the  $^1S_0 \rightarrow ^1P_1$  transition at 399 nm [28]. The MOT, located 4 mm above the substrate, is loaded with  $^{171}\text{Yb}$ ,  $^{172}\text{Yb}$ ,  $^{173}\text{Yb}$ ,  $^{174}\text{Yb}$ , or  $^{176}\text{Yb}$  atoms from an atomic beam produced by a nearby small oven, and typically contains  $5 \times 10^5$  Yb atoms at an estimated temperature of a few millikelvins.

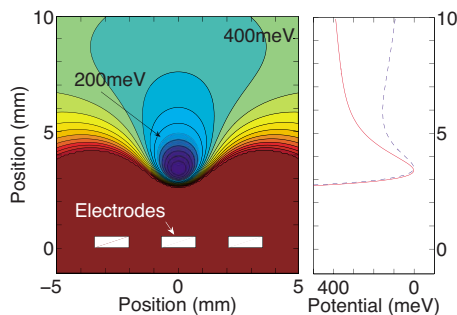


FIG. 2. (Color online) Left: Trapping pseudopotential for rf amplitudes of  $V_o = 540$  V and  $V_c = -340$  V applied to the outer and center electrodes together with a dc bias of  $-1.25$  V applied to all electrodes. The contours are spaced by 50 meV. Right: The dc-unbiased trap (dashed blue curve) exhibits less micromotion heating but is significantly shallower than the dc-biased trap (solid red curve).

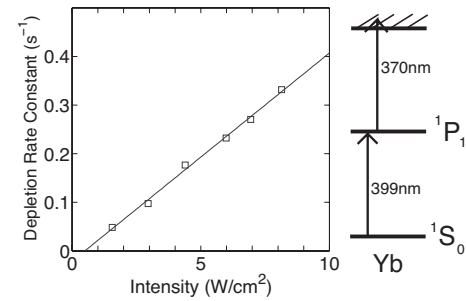


FIG. 3. Linear dependence of the loss rate constant of a  $^{174}\text{Yb}$  MOT (rms width of  $300 \mu\text{m}$ ) on 370 nm beam peak intensity ( $w = 43 \mu\text{m}$ ), indicating that photoionization is accomplished with a single 370 nm photon from the  $^1P_1$  state that is populated during laser cooling with 399 nm light.

Photoionization from the excited  $^1P_1$  state populated during laser cooling is accomplished using either the ion cooling laser at 370 nm with a power of  $750 \mu\text{W}$  and intensity of  $500 \text{ mW}/\text{cm}^2$ , or a focused uv-light-emitting diode at  $385 \pm 15$  nm with a power of 8.7 mW and intensity of  $125 \text{ mW}/\text{cm}^2$  at the MOT position. Efficient ionization is manifest as a 30% decrease in MOT atom number due to an increase in the MOT decay rate constant by  $\Gamma = 0.3 \text{ s}^{-1}$ . The generated ions are also detected directly with a Burle Magnum 5901 Channeltron avalanche detector located 4 cm above the MOT. The uv-light-induced MOT loss depends linearly on uv laser intensity (Fig. 3), indicating that the ionization process involves a single 370 nm photon. We have also confirmed that the dominant ionization proceeds from the  $^1P_1$  state: when we apply on-off modulation to both the 399 nm MOT light and the 370 nm uv light out of phase, such that the uv light interacts only with ground-state atoms, we observe a more than 13-fold decrease in ionization compared to that for in-phase modulation. From the observed loss rate in combination with an estimated saturation  $s = 0.6 - 2$  of the  $^1S_0 \rightarrow ^1P_1$  MOT transition, we determine a cross section  $\sigma = 4 \times 10^{-18} \text{ cm}^2$  for ionization of  $^{174}\text{Yb}$  with 370 nm light from the excited  $^1P_1$  state, accurate to within a factor of 2.

The photoionization typically produces  $4 \times 10^5$  cold ions per second near the minimum of the pseudopotential. Given this bright source of cold ions, trapping is easily accomplished even without ion laser cooling. We have thus trapped  $^{171}\text{Yb}^+$ ,  $^{172}\text{Yb}^+$ ,  $^{173}\text{Yb}^+$ ,  $^{174}\text{Yb}^+$ , and  $^{176}\text{Yb}^+$  ions simply by changing the MOT frequency to prepare the corresponding atomic isotopes. When searching for an initial signal with a poorly compensated trap, or to measure trap loading rates, we detect the ions after a short trapping time with the Channeltron. Since the detector electric field overwhelms the pseudopotential, we turn on the Channeltron in  $1 \mu\text{s}$  using a Pockels cell driver, fast compared to the  $3.3 \mu\text{s}$  flight time of the ions. Figure 4 shows the loading rate for photoionization of  $^{172}\text{Yb}$  atoms from the MOT and from the atomic beam for the compensated trap with a depth of  $U_0 = 0.4$  eV shown in Fig. 2. The loading rates of  $^{171}\text{Yb}^+$ ,  $^{173}\text{Yb}^+$ ,  $^{174}\text{Yb}^+$ , and  $^{176}\text{Yb}^+$  relative to  $^{172}\text{Yb}^+$  are 0.32, 0.03, 0.65, and 1.36, respectively, matching the observed MOT fluorescences. The absolute calibration of ion number in Fig. 4 has been accom-

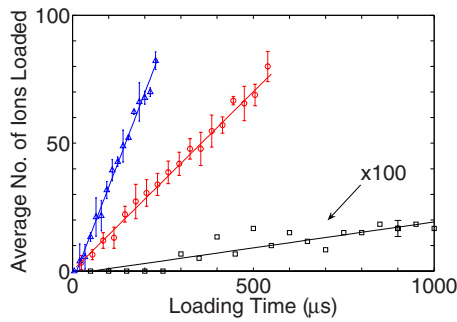


FIG. 4. (Color online) Number of trapped  $^{172}\text{Yb}$  ions for photoionization loading with the uv LED from an atomic beam (black squares), with a uv LED from a MOT (red circles), and from a MOT with both uv LED and a 370 nm laser (blue triangles). The fitted rates are  $R=200$ ,  $1.4 \times 10^5$ , and  $3.8 \times 10^5 \text{ s}^{-1}$ , respectively.

plished by comparing the Channeltron signal to the fluorescence from a known number of ions, as described below. The *loading* rate from the MOT,  $R=4 \times 10^5 \text{ s}^{-1}$ , is three orders of magnitude higher than that from the beam alone, compared to a ratio of only 4 in the ion *production* rates measured without a trap. Thus ions that were produced from laser-cooled atoms are 200 times more likely to be trapped than ions produced from the atomic beam. We ascribe this difference to the much higher MOT atomic density near the ion-trap minimum, and to the lower energy of the produced ions. As the MOT is isotopically pure, our observations of a  $10^3$  loading rate ratio between MOT and atomic beam imply an additional factor of  $10^3$  in isotope selectivity beyond the 400:1 isotope selectivity resulting from spectrally selective photoionization of an atomic beam [26].

From other work comparing electron-impact ionization and photoionization loading [25,26], we conclude that our loading rate is  $10^6$ – $10^7$  times higher than that achieved with electron-impact ionization,  $10^6$  times higher than demonstrated for other surface-electrode or microfabricated traps [11,22,23], and  $10^3$ – $10^4$  higher than in any previous experiment. By comparing the typical observed loss rate from the MOT ( $10^5 \text{ s}^{-1}$ ) to the typical ion-trap loading rate ( $2 \times 10^5 \text{ s}^{-1}$ ) under similar conditions, we conclude that our trapping efficiency for the generated ions is comparable to unity. Near-unity efficiency may help suppress anomalous ion heating that has been linked to electrode exposure to the atomic beam during the loading process [13]. The large loading rate will also be beneficial for applications that require a large, isotopically pure sample in a microfabricated trap, such as quantum simulation with an ion lattice [14].

The trapped ions are cooled and observed via fluorescence using an external-cavity grating laser [29]. To reach the target wavelength of 369.525 nm with a 372 nm laser diode (Nichia), we cool the diode to temperatures between  $-10$  and  $-20$  °C. The laser provides  $750 \mu\text{W}$  of power into a  $600\text{-}\mu\text{m}$ -diameter beam at the trap, and for initial cooling is typically tuned 150 MHz below the  $^2S_{1/2} \rightarrow ^2P_{1/2}$  transition. An external-cavity repumper laser operating at 935 nm is also necessary to empty the long-lived  $^2D_{3/2}$  state on the  $^2D_{3/2} \rightarrow ^2D[3/2]_{1/2}$  transition [30]. With cooling,  $^{172}\text{Yb}^+$  ion lifetimes in excess of 10 min were observed, limited by ei-

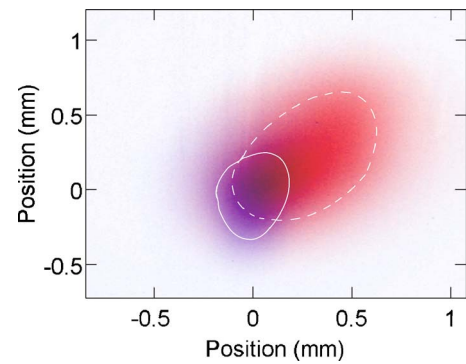


FIG. 5. (Color online) Spatially overlapping ion and atom clouds. The false color image shows a trapped  $^{172}\text{Yb}^+$  ensemble containing  $10^2$ – $10^3$  ions (blue cloud, lower left), placed inside a magneto-optical trap containing  $5 \times 10^5$  neutral  $^{172}\text{Yb}$  atoms (red cloud, upper right). The solid and dashed lines indicate the half-maximum contour for the ions and atoms, respectively.

ther laser drift or collisions with the atomic beam, compared to 5 s without laser cooling. Laser cooling of  $^{174}\text{Yb}^+$  has also been observed, while cooling of the odd isotope  $^{171}\text{Yb}^+$  would require an additional laser frequency for hyperfine repumping. The uv light scattered by the ions is collected with an aspheric lens (numerical aperture=0.4) placed inside the vacuum chamber and optimized for light gathering. The collected light passes through an interference filter and is evenly split between a charge-coupled device camera and a photomultiplier, obtaining a maximum count rate of  $5000 \text{ s}^{-1}$  per ion.

To calibrate the Channeltron detector, we first cool a small cloud of typically 100  $^{172}\text{Yb}^+$  ions to below the gas-liquid transition temperature, as identified by a small drop and subsequent strong rise in fluorescence as the laser is scanned from the long-wavelength side towards resonance [31,33]. By comparing the homogeneously broadened fluorescence of the cold cloud to that of a single trapped ion, we determine the absolute number of ions loaded and subsequently measure the Channeltron signal for the same cloud.

The optical observation of the trapped ions allows us to determine the trap position and optimize the overlap with the neutral-atom cloud. Figure 5 shows that for the optimal loading position of the trap, the pseudopotential minimum, adjusted vertically via the amplitude ratio of the rf voltages, is located inside the neutral-atom cloud. We have thus achieved simultaneous trapping of cold ions and neutral atoms in the same spatial region, which will allow the experimental investigation of cold-ion–atom collisions [17,18,20] and charge transport [19]. To study collisions beyond the current Doppler limit, the ions could be sideband cooled while the atoms could be loaded into an optical lattice [34]. The latter would also eliminate residual ion-trap loading due to MOT self-ionization.

In conclusion, we discuss a possible application of our loading technique to quantum simulation or many-ion optical clocks with signal-to-noise ratio superior to that of single-ion schemes. We consider a  $100 \times 100$  array of weakly coupled single-ion traps, to be loaded with a single isotope. At the loading rates  $R < 1 \text{ s}^{-1}$  typical of atomic-beam photoioniza-

tion loading for microfabricated traps [11], this array would take many hours to load, during which time charge-exchange collisions with the atomic beam would replace the isotope of interest with undesired ions. To address these problems, we propose a nested electrode design, where large outer electrodes provide initial trapping in the MOT region, as demonstrated in this paper, and smaller inner electrodes define the array of traps near the chip surface. A sample loaded into the

larger trap can then be transferred adiabatically into the array by varying the rf voltages supplied to the different electrodes. With the technique demonstrated here, we expect to load such an array with  $1 : 10^4$  isotope purity in less than 1 s.

We would like to thank Brendan Shields and Ken Brown for assistance. This work was supported in part by the NSF Center for Ultracold Atoms.

- 
- [1] P. Zoller *et al.*, *Eur. Phys. J. B* **36**, 204 (2005).  
 [2] C. Monroe, D. M. Meekhof, B. E. King, W. M. Itano, and D. J. Wineland, *Phys. Rev. Lett.* **75**, 4714 (1995).  
 [3] D. Kielpinski, V. Meyer, M. A. Rowe, C. A. Sackett, W. M. Itano, C. Monroe, and D. J. Wineland, *Science* **291**, 1013 (2001).  
 [4] M. D. Barrett *et al.*, *Nature (London)* **429**, 737 (2004).  
 [5] M. Riebe *et al.*, *Nature (London)* **429**, 734 (2004).  
 [6] D. Leibfried *et al.*, *Nature (London)* **438**, 639 (2005).  
 [7] H. Haeffner *et al.*, *Nature (London)* **438**, 643 (2005).  
 [8] P. W. Shor, *Phys. Rev. A* **52**, R2493 (1995).  
 [9] A. M. Steane, *Phys. Rev. Lett.* **77**, 793 (1996).  
 [10] J. Chiaverini *et al.*, *Quantum Inf. Comput.* **5**, 419 (2005).  
 [11] D. Stick, W. Hensinger, S. Olmschenk, M. Madsen, K. Schwab, and C. Monroe, *Nat. Phys.* **2**, 36 (2006).  
 [12] B. DeMarco *et al.*, *Quantum Inf. Comput.* **5**, 419 (2005).  
 [13] L. Deslauriers, S. Olmschenk, D. Stick, W. K. Hensinger, J. Sterk, and C. Monroe, *Phys. Rev. Lett.* **97**, 103007 (2006).  
 [14] D. Porras and J. I. Cirac, *Phys. Rev. Lett.* **93**, 263602 (2004).  
 [15] W. H. Oskay *et al.*, *Phys. Rev. Lett.* **97**, 020801 (2006).  
 [16] M. Keller, B. Lange, K. Hayasaka, W. Lange, and H. Walther, *Nature (London)* **431**, 1075 (2004).  
 [17] R. Côté and A. Dalgarno, *Phys. Rev. A* **62**, 012709 (2000).  
 [18] O. Makarov, R. Côté, H. Michels, and W. W. Smith, *Phys. Rev. A* **67**, 042705 (2003).  
 [19] R. Côté, *Phys. Rev. Lett.* **85**, 5316 (2000).  
 [20] W. W. Smith, O. P. Makarov, and J. Lin, *J. Mod. Opt.* **52**, 2253 (2005).  
 [21] R. Côté, V. Kharchenko, and M. Lukin, *Phys. Rev. Lett.* **89**, 093001 (2002).  
 [22] S. Seidelin *et al.*, *Phys. Rev. Lett.* **96**, 253003 (2006).  
 [23] K. R. Brown *et al.*, *Phys. Rev. A* **75**, 015401 (2007).  
 [24] N. Kjaergaard *et al.*, *Appl. Phys. B: Lasers Opt.* **71**, 207 (2000).  
 [25] C. Balzer, A. Braun, T. Hannemann, C. Paape, M. Ettler, W. Neuhauser, and C. Wunderlich, *Phys. Rev. A* **73**, 041407(R) (2006).  
 [26] D. M. Lucas *et al.*, *Phys. Rev. A* **69**, 012711 (2004).  
 [27] M. Keller, B. Lange, and K. Hayasaka, *J. Phys. B* **36**, 613 (2003).  
 [28] C. Y. Park and T. H. Yoon, *Phys. Rev. A* **68**, 055401 (2003).  
 [29] D. Kielpinski, M. Cetina, J. A. Cox, and F. X. Kärtner, *Opt. Lett.* **31**, 757 (2005).  
 [30] A. S. Bell, P. Gill, H. A. Klein, A. P. Levick, C. Tamm, and D. Schnier, *Phys. Rev. A* **44**, R20 (1991).  
 [31] F. Diedrich, E. Peik, J. Chen, W. Quint, and H. Walther, *Phys. Rev. Lett.* **59**, 2931 (1987).  
 [32] Y. C. Chen *et al.*, *Phys. Rev. Lett.* **93**, 265003 (2004).  
 [33] L. Hornekaer and M. Drewsen, *Phys. Rev. A* **66**, 013412 (2002).  
 [34] Y. Takasu *et al.*, *Phys. Rev. Lett.* **91**, 040404 (2003).